How do weather characteristics change in a warming climate?

Ok-Yeon Kim, Bin Wang & Sun-Hee Shin

Climate Dynamics
Observational, Theoretical and Computational Research on the Climate System

ISSN 0930-7575
Volume 41
Combined 11-12

Clim Dyn (2013) 41:3261-3281
DOI 10.1007/s00382-013-1795-8

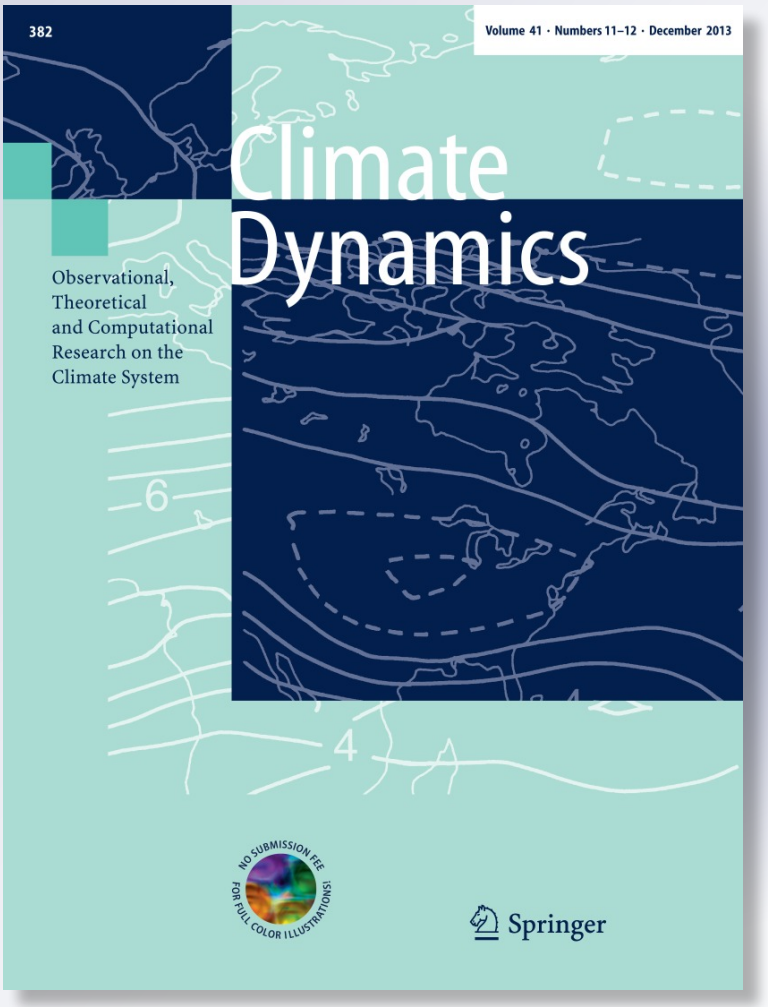

Springer

Clim Dyn (2013) 41:3261–3281
DOI 10.1007/s00382-013-1795-8

How do weather characteristics change in a warming climate?

Ok-Yeon Kim · Bin Wang · Sun-Hee Shin

Received: 31 July 2012 / Accepted: 29 April 2013 / Published online: 8 May 2013

Abstract The possible change in the characteristics of weather in the future should be considered as important as the mean climate change because the increasing risk of extremes is related to the variability on daily time scales. The weather characteristics can be represented by the climatological mean interdiurnal (day-to-day) variability (MIDV). This paper first assessed the phase five of the Coupled Model Intercomparison Project coupled climate models' capability to represent MIDV for the surface maximum and minimum temperature, surface wind speed and precipitation under the present climate condition. Based on the assessment, we selected three best models for projecting future change. We found that the future changes in MIDV are characterized by: (a) a marked reduction in surface maximum and minimum temperature over high latitudes during the cold season; (b) a stronger reduction in the surface minimum temperature than in the maximum temperature; (c) a reduction in surface wind speed over large parts of lands in Northern Hemisphere (NH) during NH spring; (d) a noticeable increase in precipitation in NH mid-high latitudes in NH spring and winter, and in particular over East Asia throughout most of the year.

O.-Y. Kim (✉) · S.-H. Shin
APEC Climate Center (APCC), 12 Centum 7-ro, Haeundae-gu, Busan 612-020, Republic of Korea
e-mail: oykim@apcc21.org

S.-H. Shin
e-mail: ssh222@apcc21.org

B. Wang
Department of Meteorology, International Pacific Research Center (IPRC), University of Hawaii, Honolulu, HI 96822, USA
e-mail: wangbin@hawaii.edu

Keywords Mean interdiurnal variability · Extreme events · Climate change · Weather characteristics · CMIP5

1 Introduction

Climate models have long been subjected to various tests to evaluate their performances in simulating and improving our understanding of climate variability and change. In particular, a series of phases of the Coupled Modeling Intercomparison Project (CMIP) have been designed to support climate model diagnosis, validation and intercomparison in a systematic way. Since the framework of the first phase of CMIP (CMIP1) was established in 1995, various systematic and comprehensive efforts have been made to understand and attribute climate change (e.g., IPCC 2007).

Accurate simulation of one climate facet does not necessarily mean an accurate representation of other facets, and it is therefore crucial to evaluate a broad spectrum of climate processes and phenomena in climate models (Gleckler et al. 2008; Pincus et al. 2008; Taylor 2001). In this study we focus on the interdiurnal (day-to-day) variability as an aspect of climate because: (1) There is a good representation of second-order moments (variability) on various time scales (e.g., interdiurnal, intraseasonal or interannual), which is as critical as the first-order moments (climatological means) in climate model assessment (Scherrer 2011); (2) there have been few studies on interdiurnal atmospheric variability in comparison with those focused on longer (e.g., intraseasonal or interannual) time scales (Kitoh and Mukano 2009); and (3) this research is expected to contribute to many climate-related application sectors which intrinsically rely on an accurate representation of daily-scale variability (Prudhomme et al. 2002).

Before the daily output from model simulations became available, research was predominantly devoted to the investigation of the interdiurnal variability of surface temperature over a specific area using observations (e.g., Driscol et al. 1994; Rosenthal 1960; Williams and Parker 1997). Most of this research concentrated on the United States and the North Atlantic Ocean, where there was an accessible dataset incorporating a long period of records.

In terms of model simulations, few studies have been conducted on the importance of considering the effects of interdiurnal variability on either regional or global climate change. In addition, the majority of studies have been based only on the interdiurnal variability of surface-air temperature. According to Cao et al. (1992), a single model simulation for the present climate demonstrated that the pattern and magnitude of simulated day-to-day variability of surface temperature were generally similar to those of observed. However, on the doubled CO_2 level, the model simulated a marked reduction in the day-to-day variability of surface temperature (Cao et al. 1992). Changes in daily surface temperature variability were also investigated by using multiple global (Kitoh and Mukano 2009), or regional (Fischer and Schär 2009) climate model scenarios and future daily surface temperature variability was projected to increase over land in the Northern Hemisphere summer and in the tropics (Kitoh and Mukano 2009). On a regional scale, daily summer temperature variability was also projected to increase over France (Fischer and Schär 2009).

Recently, extensive daily dataset from multiple global model simulation scenarios have been made available through CMIP5 (cf. Taylor et al. 2012). This abundant dataset makes it possible to evaluate the daily variability for not only surface temperature but also many other surface variables such as wind speed and precipitation. It also enables the investigation of future changes in their daily variability by using multi-model ensemble projections.

Our objective in this study was to investigate whether the future global climate would get better or worse. Surface maximum and minimum temperature, surface wind speed and precipitation are susceptible variables in our lives and can affect, among other factors, the wind-chill temperature. An increase in the interdiurnal variability of the surface climate would be detrimental to our comfort, and conversely, a projected decrease in the interdiurnal variability of the surface climate; would be beneficial. To accomplish our purpose, we first examined; (1) how the observed interdiurnal variability of surface maximum and minimum temperature, surface wind speed and precipitation is represented in a reanalysis dataset, (2) how efficiently the CMIP5 multi-models resolve observed interdiurnal variability in the present climate: which models showed a greater capability to represent interdiurnal variability, and thus which models would be preferred for use in projecting future changes; and (3) the projected changes in interdiurnal variability in the future climate by the most reliable CMIP5 models. Through this study, we expected to gain knowledge of the possible features of future weather conditions under a warming climate induced by the new developed emission scenarios of the CMIP5 projects.

The outline of the paper is as follows. First, we described reanalysis and model dataset used in this study (Sect. 2) followed by methods used for the analysis (Sect. 3). Section 4 presented the results of our analysis: interdiurnal variability from reanalysis (Sect. 4.1) and multi global climate models (Sect. 4.2–4.3). In Sect. 4.2, we assessed models' performance in simulating interdiurnal variability in the present climate, and in Sect. 4.3 we discussed future interdiurnal variability from models' projection. The paper was concluded by a summary in Sect. 5.

2 Reanalysis and models

2.1 Reanalysis

We considered two reanalysis datasets: National Centers for Environmental Prediction (NCEP)–National Center for Atmospheric Research (NCAR) Reanalysis II (Kanamitsu et al. 2002; hereinafter NCEP-R2) and European Center for Medium range Weather Forecasting (ECMWF) ERA-Interim reanalysis (Dee et al. 2011; hereinafter ERA-Interim). We also used one global precipitation dataset named Global Precipitation Climatology Project dataset (Yin et al. 2004; Huffman et al. 2001; Bolvin et al. 2009; hereinafter GPCP). Using the datasets, we focused on four daily life-sensitive surface variables; i.e., daily maximum and minimum near surface (2-m) air temperature, daily near surface (10-m) wind speed and daily precipitation.

NCEP-R2 is the only dataset that provides daily maximum and minimum temperature: ERA-Interm provides only daily mean temperature. Since both NCEP-R2 and ERA-Interim showed similar interdiurnal variability in daily surface mean temperature (not shown), we decided to use NCEP-R2 dataset for surface maximum and minimum temperature extending from 1979 to 2005 (27 years). The results obtained can infer interdiurnal variability in daily mean temperature.

We also compared MIDV from 1979 to 2005 in surface wind speed computed from NCEP-R2 and Era-Interim. In general, NCEP-R2 presented higher interdiurnal variability over the land and ocean compared to that in Era-Interim (not shown); however, Szczypta et al. (2011) found that ERA-Interim reasonably reproduced the observed surface wind speed. Therefore, we selected ERA-Interim dataset for surface wind speed.

Table 1 Summary of CMIP5 models used in this study

Index	Organization/countries	Model identification	Atmosphere resolution	Ocean resolution	Number of ensembles	
					Present	RCP4.5
A	CSIRO, BOM/Australia	ACCESS1-0	1.875 × 1.25 × 38	1.0 × 1.0L50	1	1
B	BCC/China	bcc-csm1-1	T42L26	1.0 × (1–1/3)L40	3	1
C	CCCma/Canada	CanESM2	T63L35	256 × 192L40	5	3
D	CSIRO –QCCCE/Australia	CSIRO-Mk3-6-0	T63L18	1.875 × 0.9375L31	10	10
E	NOAA, GFDL/USA	GFDL-ESM2G	M45L24	360 × 210L63	2	1
F	MOHC/UK	HadGEM2-CC	N96L60	(1.0–0.3) × 1.0L40	1	1
G	MOHC/UK	HadGEM2-ES	N96L38	(1.0-0.3) × 1.0L40	1	1
H	INM/Russia	INM-CM4	2.0 × 1.5 × 21	1.0 × 0.5 × 40	1	1
I	IPSL/France	IPSL-CM5A-LR	96 × 95 × 39	2 × 2L31	1	2
J	IPSL/France	IPSL-CM5A-MR	144 × 143 × 39	2 × 2L31	1	1
K	AORI, NIES, JAMSTEC/Japan	MIROC5	T85L40	256 × 224L5	4	3
L	AORI, NIES, JAMSTEC/Japan	MIROC-ESM	T42L80	256 × 192L44	3	1
M	AORI, NIES, JAMSTEC/Japan	MIROC-ESM-CHEM	T42L80	256 × 192L44	1	1
N	MPI-M/Germany	MPI-ESM-LR	T63L47	GR15L40	3	3
O	MRI/Japan	MRI-CGCM3	TL159L48	1 × 0.5L51	5	1

A comparison of interdiurnal variability from 1979 to 2005 in precipitation calculated from NCEP-R2 and ERA-Interim revealed large disagreement among the magnitude of interdiurnal variability. Because of the large difference, we also computed interdiurnal variability from 1997 to 2005 (9 years) in precipitation using GPCP and the reanalysis. Again, the magnitude of interdiurnal variability in precipitation calculated from GPCP appeared different from those computed from other reanalysis. Therefore, we decided to use GPCP dataset for daily precipitation ranging from 1997 to 2005. For a fare comparison, we selected the length of coverage of the CMIP5 models to match the corresponding time-periods of observations. Gebremichael et al. (2005) found that (1) GPCP daily product captured well the variability of precipitation, and (2) the GPCP daily dataset can realistically detect rainy days at a large range of thresholds. Bolvin et al. (2009) also concluded that GPCP dataset captured fairly well the day-to-day occurrence of precipitation and the GPCP daily fields are useful for meteorological and hydrological studies to some extent.

Note that daily variables from two reanalysis datasets and the global precipitation dataset are interpolated onto 1.875° (longitude) by 1.875° (latitude) in order to compare the daily variables with those from multi-models.

2.2 Models

We used the daily output from 15 CMIP5 models. Daily outputs of the models used in this study were analyzed for three time slices: historical simulations of contemporary

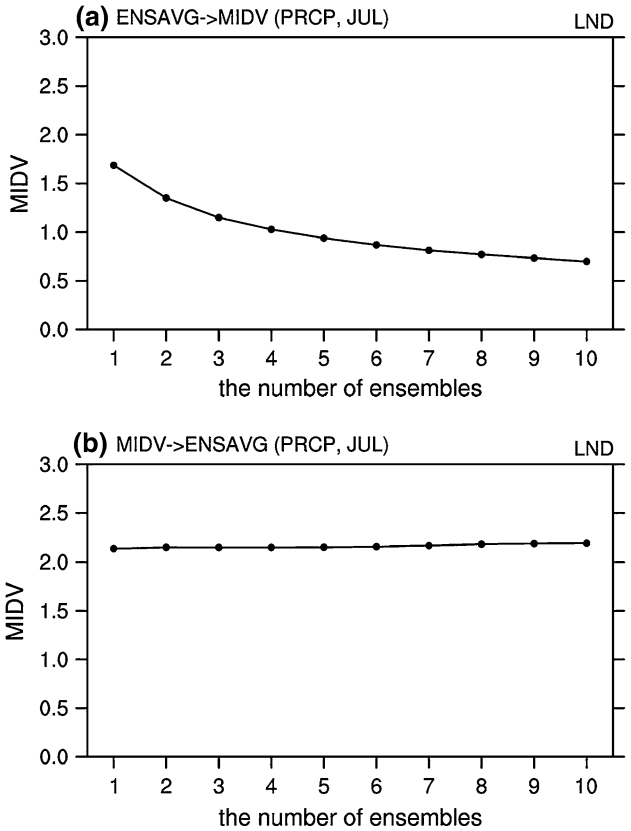

Fig. 1 Global land weighted averaged MIDV as a function of the number of ensembles using CSIRO-Mk3-6-0 model: **a** averaging with different number of ensembles for precipitation, then calculating MIDV and **b** calculating MIDV in precipitation from individual ensembles, then averaging with different number of ensembles

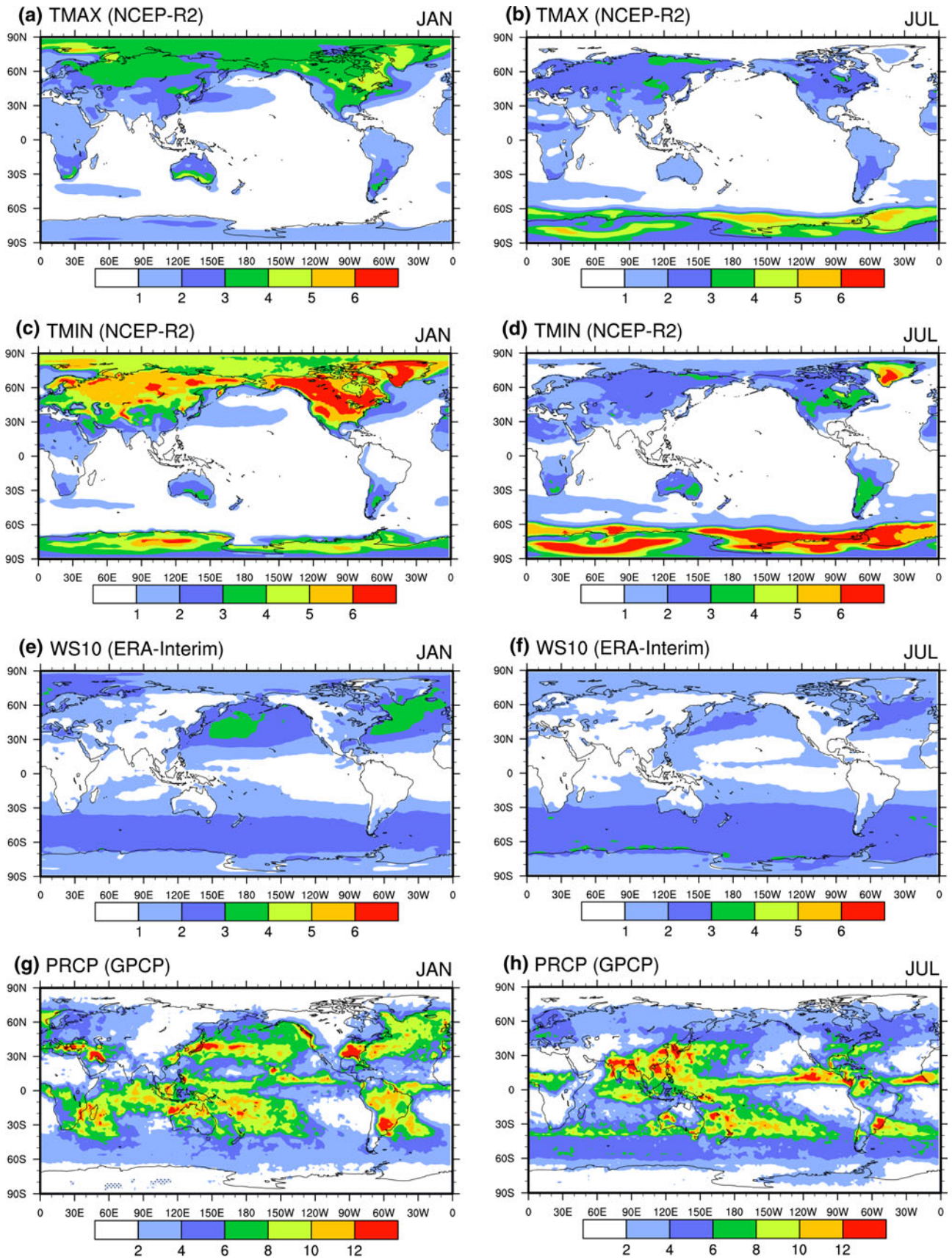

◀**Fig. 2** Observed MIDV in the reanalysis dataset: **a**, **b** surface maximum temperature (K) from NCEP–NCAR reanalysis 2, **c**, **d** surface minimum temperature (K) from NCEP-NCAR reanalysis 2, **e**, **f** surface wind speed (m/s) from ERA-Interim reanalysis and **g**, **h** precipitation (mm/day) from GPCP. Note that the dataset for daily precipitation from GPCP ranges from 1997 to 2005 (9 years), and the datasets for other variables extends from 1979 to 2005 (27 years)

climate (1979–2005; hereinafter "Present"); one of the RCP (Representative Concentration Pathways) scenario simulations of future climate (2030–2056 and 2073–2099; hereinafter "RCP4.5"). The latter two experiments are long-term (century time-scale) simulations, initialized from the end of freely evolving simulations of the historical period under the CMIP5 strategy (Hibbard et al. 2007; Meehl and Hibbard 2007). For the historical simulations, changing conditions consistent with observation were additionally imposed by including atmospheric composition (including CO_2), solar forcing, emissions or concentrations of short-lived species and natural and anthropogenic aerosols and land use (Taylor et al. 2012). The RCP4.5 scenario used in this study is a stabilization scenario in which radiative forcing is stabilized at 4.5 Wm^{-2} in 2100 and radiative forcing and CO_2 concentrations are held constant after 2100 (Clarke et al. 2007; Smith and Wigley 2006; Wise et al. 2009).

The 15 CMIP5 models evaluated in this study come from nearly all the major climate modeling groups and are detailed in Table 1. As in the case of the reanalysis datasets, we employed daily variables including maximum and minimum near surface (2-m) air temperature, near surface (10-m) wind speed and precipitation from the 15 models. Because all models have different spatial resolutions, each variable from each ensemble, model and experiment was interpolated onto the 1.875° (latitude) by 1.875° (longitude) as performed with the reanalysis and global precipitation datasets.

Since each model has a different number of ensembles for each experiment, the treatment of the ensembles in a specific model is an issue. Given that the interdiurnal (day-to-day) variability that we addressed in this study is largely an expression of '*internal variability*' and, therefore, it will not be in phase across ensemble, the ensemble averaging before the interdiurnal variability is calculated will greatly reduce the computed interdiurnal variability. Figure 1 supported this hypothesis: we compared global land-only areal weighted averaging of interdiurnal variability (the definition will be given in Sect. 3.1) as a function of the number of ensembles using CSIRO-Mk3-6-0 model which has the most number of ensembles. Figure 1a showed the result of averaging with different number of ensembles for precipitation in July, and then calculating interdiurnal variability, and Fig. 1b displayed the result of calculating interdiurnal variability in precipitation in July from each of individual ensembles, and then averaging with different number of ensembles. Averaging with more ensemble members for precipitation in a specific model significantly reduced the calculated interdiurnal variability in precipitation (Fig. 1a). On the other hand, averaging with more ensemble members' interdiurnal variability in precipitation was insensitive to the number of ensemble members (Fig. 1b). The magnitude of interdiurnal variability was even larger than that in Fig. 1a. Therefore, an appropriate approach to deal with different number of ensembles in calculation of interdiurnal variability would be to first calculate interdiurnal variability from each individual ensemble member and then calculate the ensemble average in a specific model.

3 Methods

3.1 Definition of mean interdiurnal variability (MIDV)

The interdiurnal variability (day-to-day variation) of a variable denotes the magnitude of the difference in the daily variable between two consecutive days and is abbreviated to "IDV". By averaging the IDV over the entire period for a particular month, we obtained the mean interdiurnal variability (abbreviated as "MIDV"). The interdiurnal variability was calculated by subtracting the value of one day from that of the following day. Those daily differences were then converted to absolute values, which express the magnitude of daily change, regardless of the sign of the change. Williams and Parker (1997) stated that the absolute value of IDV captures the chronological sequence of variable change throughout a month, but the use of standard deviations or similar measures of variability, does not. Finally, by averaging the absolute value of IDV over all the years for a particular month, we found MIDV. Mathematically, the IDV and MIDV are defined by the following (1) and (2) respectively:

$$\mathrm{IDV}_{\mathrm{X}}^{\mathrm{i,j}}(\mathrm{m},\mathrm{y}) = \frac{1}{N-1}\sum_{d=1}^{N-1}\mathrm{abs}\left(\mathrm{X}_{\mathrm{d+1}}^{\mathrm{i,j}}(\mathrm{m},\mathrm{y}) - \mathrm{X}_{\mathrm{d}}^{\mathrm{i,j}}(\mathrm{m},\mathrm{y})\right) \tag{1}$$

where X indicates each variable considered; i and j denote each grid point; and d, m, y and N represent day, month, year and the number of days of a month, respectively.

$$\mathrm{MIDV}_{\mathrm{X}}^{\mathrm{i,j}}(\mathrm{m}) = \frac{1}{\mathrm{n}}\sum_{\mathrm{y}=1}^{\mathrm{n}}\mathrm{IDV}_{\mathrm{X}}^{\mathrm{i,j}}(\mathrm{m},\mathrm{y}) \tag{2}$$

where n means the number of years. As a result, we attained two-dimensional fields of MIDV for each variable for a particular month. The same terms and their definitions

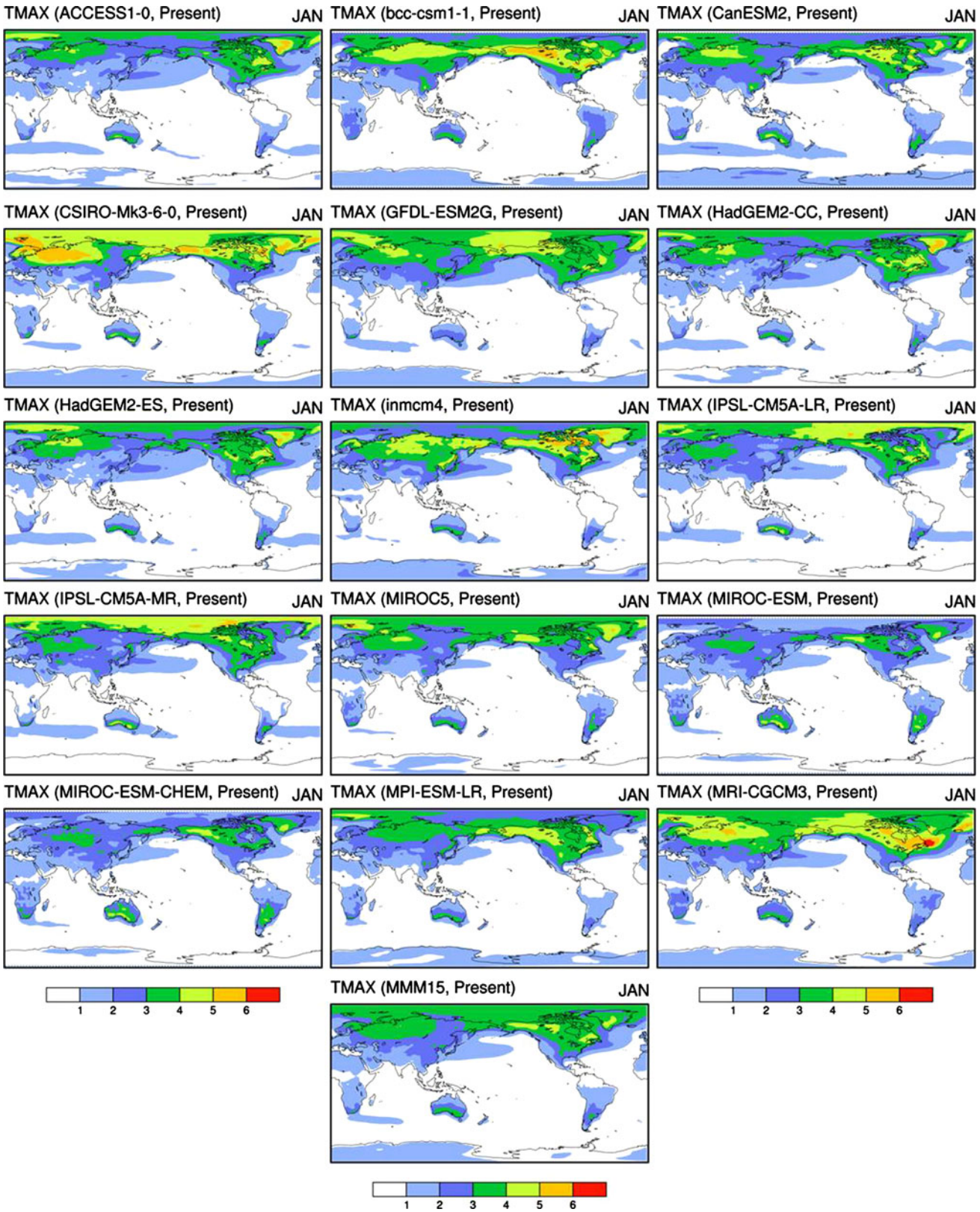

Fig. 3 Simulated MIDV in surface maximum temperature (K) in January for 27 years from 1979 to 2005 calculated from 15 CMIP5 models and MMM15

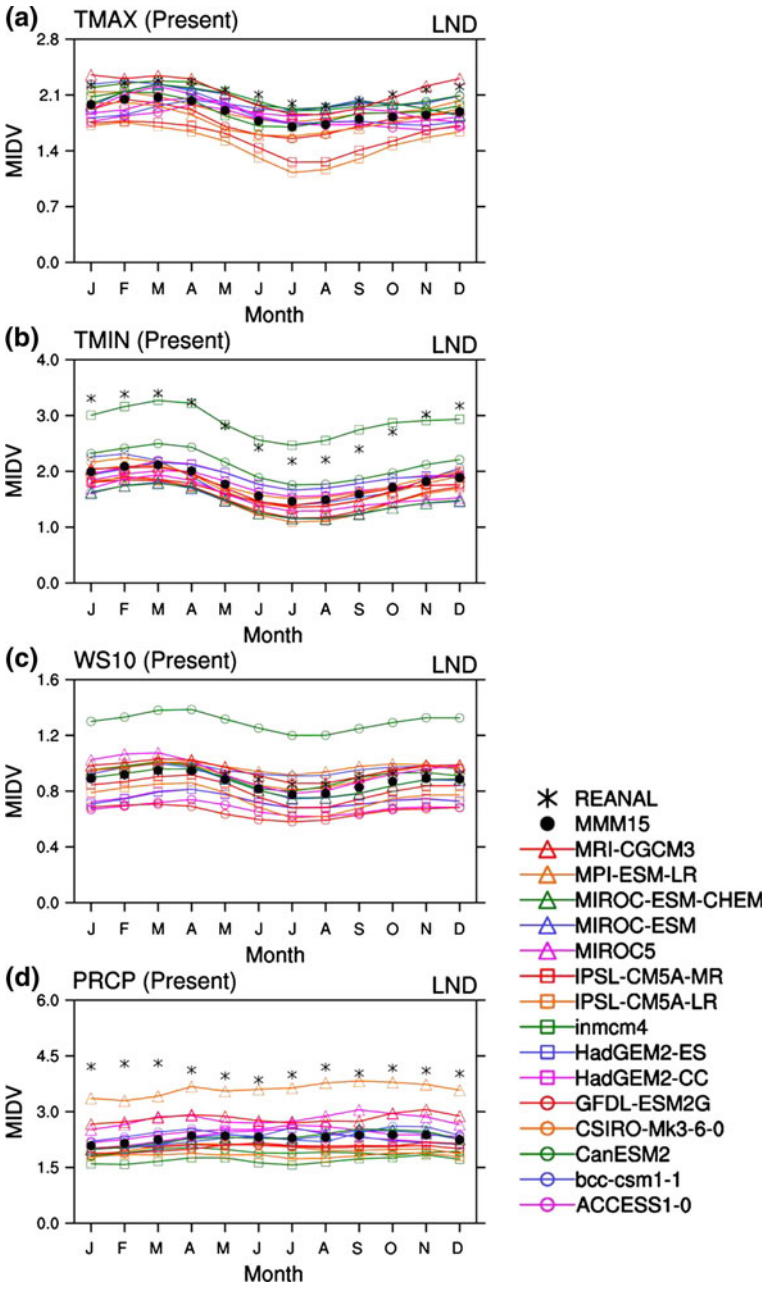

Fig. 4 Annual cycle of area-averaged MIDV for **a** surface maximum temperature (K), **b** surface minimum temperature (K), **c** surface wind speed (m/s) for 27 years from 1979 to 2005 and **d** precipitation (mm/day) for 9 years from 1997 to 2005 calculated from reanalysis (*asterisks*), 15 CMIP5 models (*colored lines* with *symbols*) and MMM15 (*black dots*). Note that the MIDV over land only is considered for calculation of the area-averaged mean

are used in literature (Driscol et al. 1994; Rosenthal 1960; Williams and Parker 1997).

3.2 Metrics for assessing MIDV

In this study, metrics are constructed to justify the models' performances in representing observed MIDV for the maximum and minimum surface air temperature, near surface wind speed and precipitation. In developing the metrics for evaluating the MIDV from the models' simulations against those from reanalysis datasets, we computed two statistical summaries: the pattern correlation coefficient (PCC) and the root mean square error (RMSE). We also introduced a statistical measure called the variability index (VI) for each model, variable and grid-point:

$$\mathrm{VI}_{\mathrm{X}}^{\mathrm{i,j}}(\mathrm{m}) = \left(\sqrt{\frac{\mathrm{MIDV}_{\mathrm{X}}^{\mathrm{i,j}}(\mathrm{m})}{\mathrm{MIDV}_{\mathrm{X,ref}}^{\mathrm{i,j}}(\mathrm{m})}} - \sqrt{\frac{\mathrm{MIDV}_{\mathrm{X,ref}}^{\mathrm{i,j}}(\mathrm{m})}{\mathrm{MIDV}_{\mathrm{X}}^{\mathrm{i,j}}(\mathrm{m})}} \right)^2 \quad (3)$$

where $\mathrm{MIDV}_{\mathrm{X}}^{\mathrm{i,j}}(\mathrm{m})$ and $\mathrm{MIDV}_{\mathrm{X,ref}}^{\mathrm{i,j}}(\mathrm{m})$ are the two-dimensional MIDV of the model and reference for each variable, X, for a particular month, m. Based on the definition of VI, the value of VI is always positive and unbounded above. Smaller values of VI indicate a better agreement with the

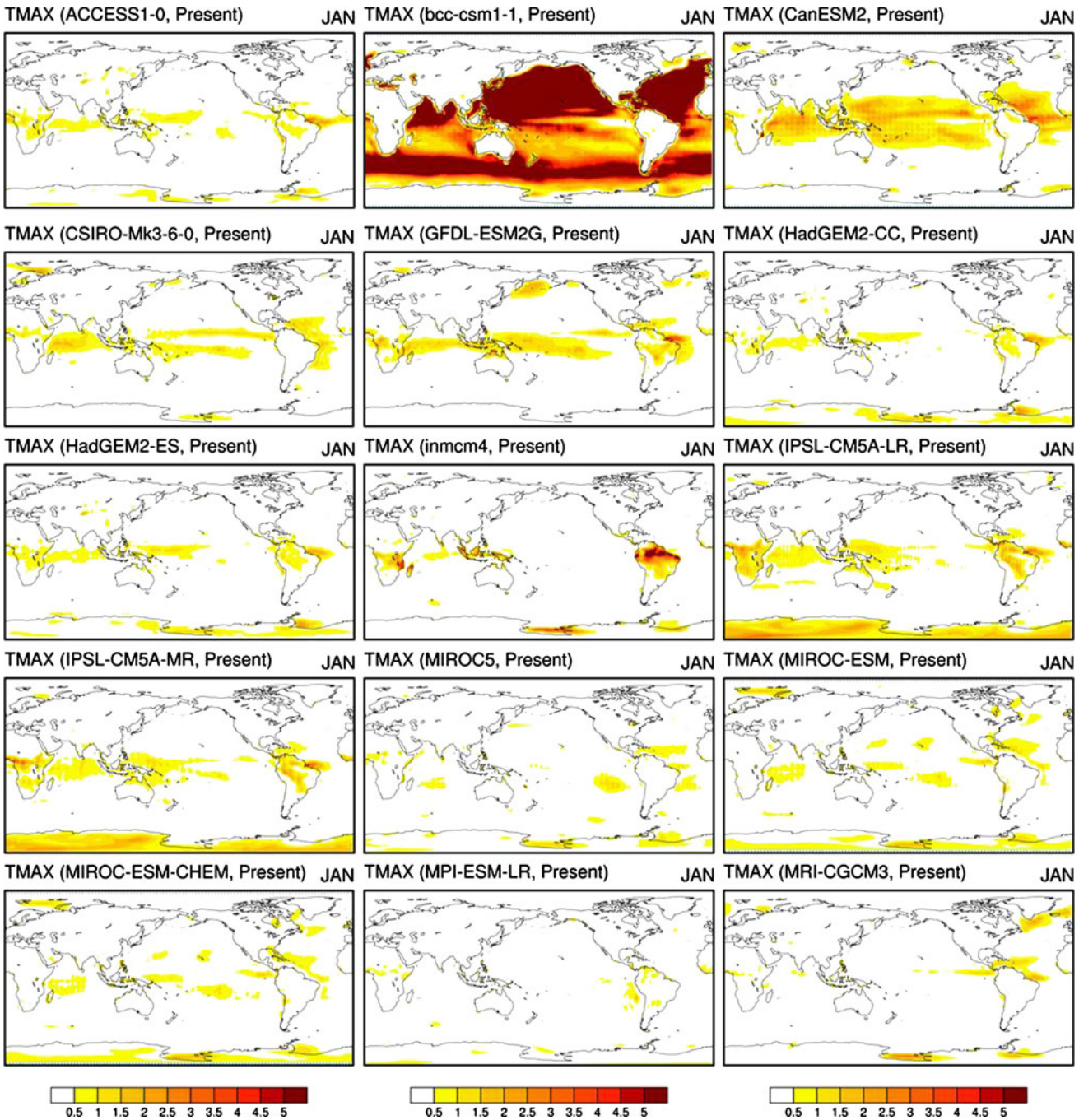

Fig. 5 VI for surface maximum temperature (K) in January calculated for 27 years from 1979 to 2005 using 15 CMIP5 models and reference datasets (reanalysis). Note that areas in *dark red* indicate a large departure from the reference datasets and vice versa

reference dataset; a perfect agreement between model and reference dataset would result in 0 of VI. The basic concept of this measure is closely related to that of the quantity used by Gleckler et al. (2008) and Scherrer (2011), in which they used the standard deviation of the seasonal value instead of the MIDV of the daily value. The VI is a good measure in assessing the differences in MIDV between the model and the reference dataset; enabling us to identify consistent biases in the MIDV of a single model.

Using the metrics (consisting of PCC, RMSE and VI) calculated for each model, we examined how well the CMIP5 models can resolve the MIDV in the present climate. In addition, based on the metrics, we determined which models among the 15 CMIP5 models could be selected for projecting future changes in MIDV in the future climate. Note that the metrics presented in this study to compare the model and reanalysis results involve the area-weighted average of a quantity. The area represented

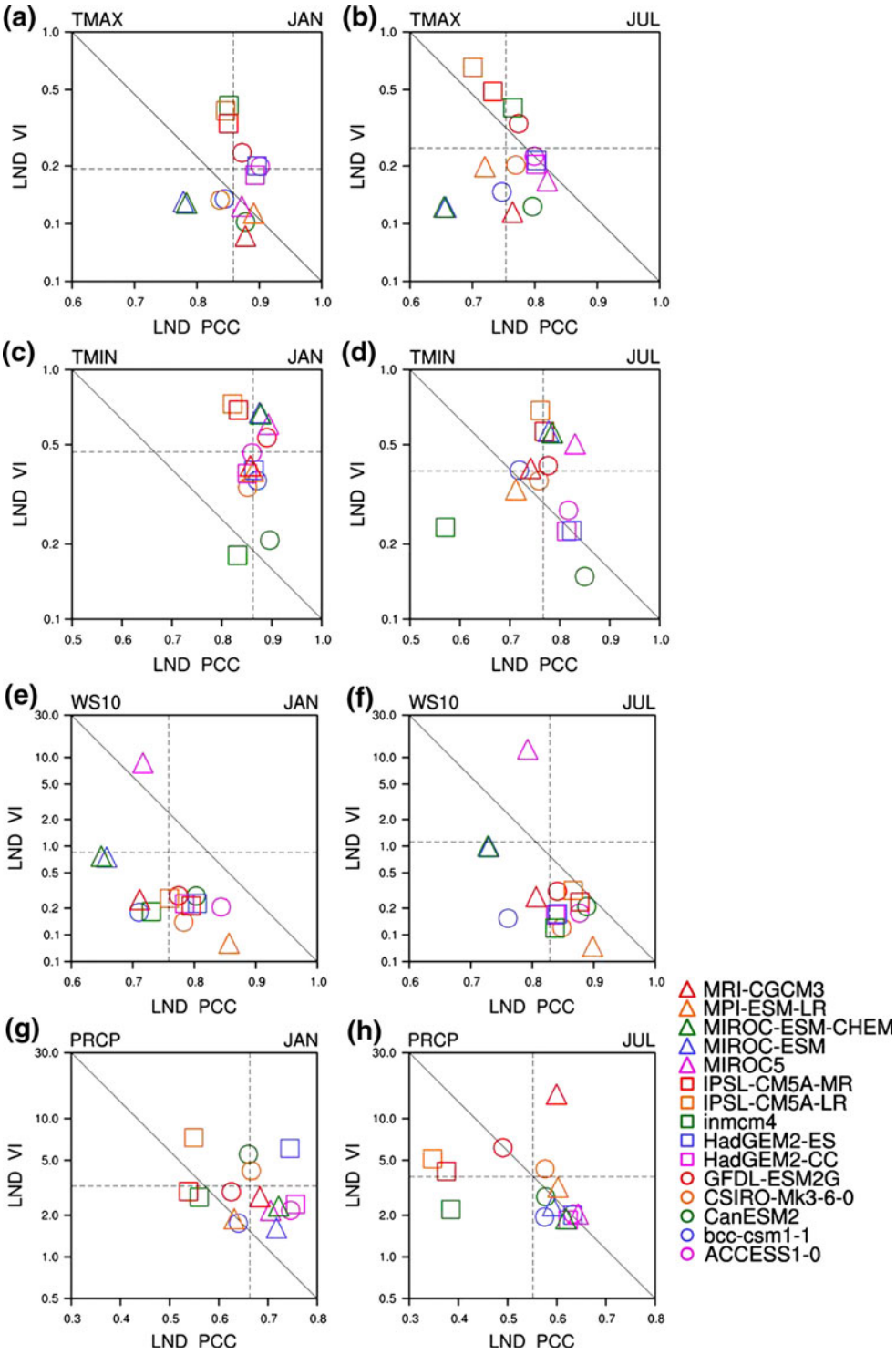

Fig. 6 Scatter diagrams showing VI versus PCC from each CMIP5 model averaged over lands only: **a**, **b** surface maximum temperature, **c**, **d** surface minimum temperature and **e**, **f** surface wind speed ranging from 1979 to 2005 (27 years) and **g**, **h** precipitation extending from 1997 to 2005 (9 years). *Dashed lines* indicate the median value of a models' VI or PCC, and *solid lines* are diagonals. Note that the scale is logarithmic on the y-axis

by each grid point is a function of latitude (i.e., cosine of latitude).

3.3 Signal-to-noise (SN) ratio of MIDV

It is well known that uncertainty about how the future climate will change stems mainly from results presented by the internal variability of models, and the models' responses to increased radiative forcing and to forcing itself (Deser et al. 2012; IPCC 2007). These uncertainties play a significant role in determining a signal-to-noise (SN) ratio of climate change, which is considered a critical factor for climate impact studies (e.g., Santer et al. 2011). The SN ratio is defined as the multi-model mean changes

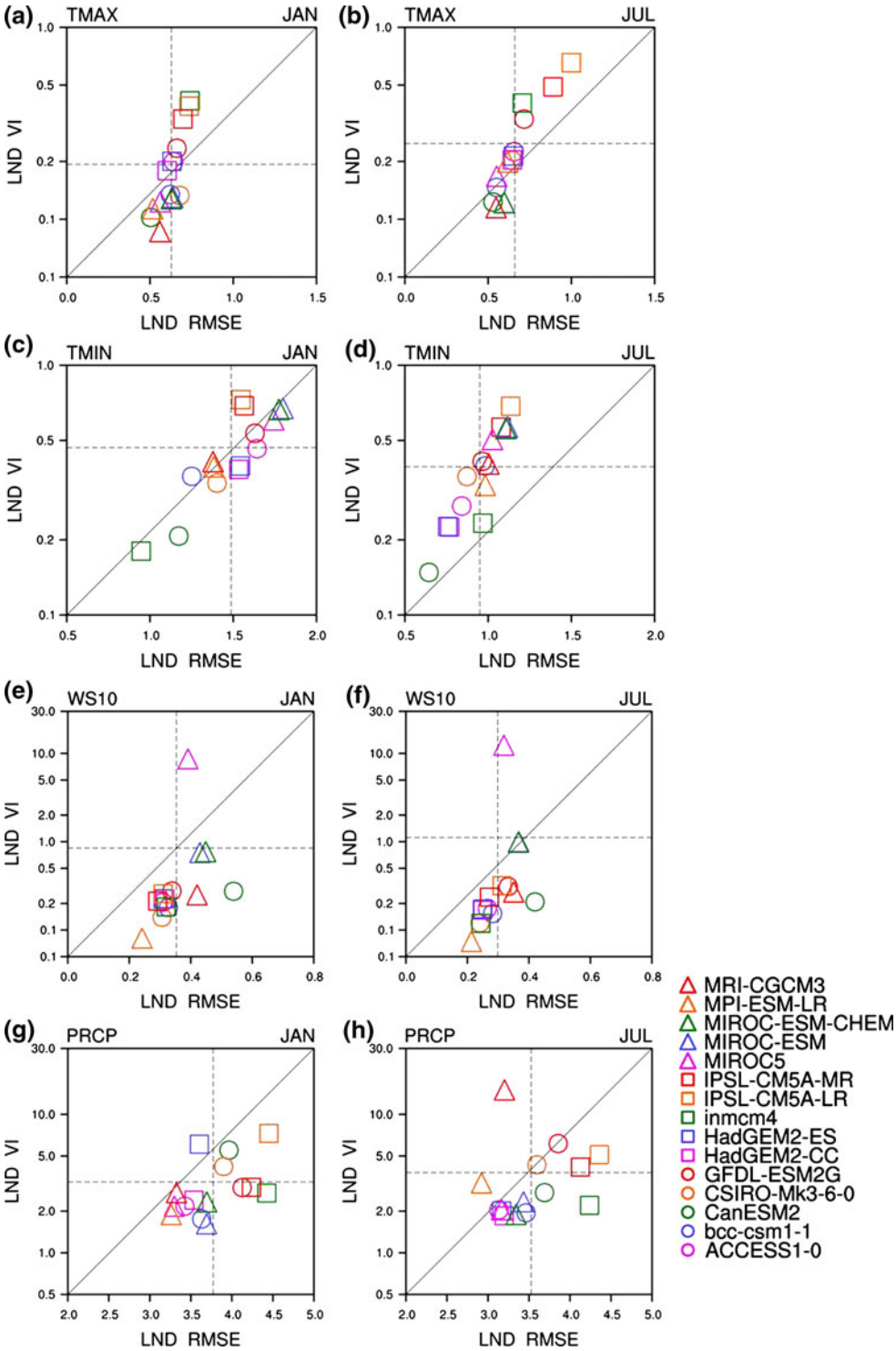

Fig. 7 Same as Fig. 6 except for scatter diagram showing VI versus RMSE

for the RCP4.5 simulation for the future period (2030–2056 and 2073–2099) relative to historical simulation for the base period (1979–2005) divided by inter-model standard deviation of the changes. The quantity we examined is climatological mean interdiurnal variability (MIDV). This quantity is relatively stable among different models because they are large sample mean values. Even with three best models (see Sect. 4.2.2) the model spreads (inter-model standard deviations) at each grid points are relatively steady and spatially consistent. Thus, absolute values of ratios higher than 1 indicates a dominance of signal over noise and those lower than 1 indicates a dominance of noise over signal. Calculating the SN ratio, we assessed how CMIP5 models are able to project the changes in

MIDV in the future climate and identified how much confidence we would expect in our future projections for MIDV. That is, the SN ratio is used here to quantify climate change uncertainty for a prescribed RCP scenario (e.g., Lobell et al. 2007).

4 Results

4.1 Observed MIDV

In examining the observed MIDV for maximum and minimum temperature calculated from NCEP-R2, we found a larger MIDV over the extratropical winter hemisphere (Fig. 2a–d). In January, the MIDV is about 3–4 K (higher than 4 K over the northeast North America) for maximum temperature and 4–6 K (higher than 6 K over the North America, Canada, Alaska and Greenland) for minimum temperature over land higher than 50° N. In July, the MIDV for maximum temperature is high in the Antarctic and that for minimum temperature is high in the Antarctic and Alaska. This result is in good agreement with previous studies. The MIDV for temperature should be the largest in the cold season when advective temperature changes are most intense and smallest in the warm season when advective temperature changes are least intense (Rosenthal 1960). In addition, the MIDV for minimum temperature is larger than that of maximum temperature.

In analyzing MIDV for surface wind speed (Fig. 1e, f), we found that the MIDV is the smallest over the tropics and largest over the ocean in the extratropics. In particular, the maximum value of MIDV is found over the North Pacific and North Atlantic Ocean in NH winter. In addition, the MIDV is much stronger in the cold season than in the warm season. We also explored MIDV for precipitation (Fig. 1g–h). A larger value of MIDV for precipitation is found along the Intertropical Convergence Zone (ITCZ) and winter storm tracks. The MIDV in NH summer is also larger in the monsoon regions including Southern Asia, South-east Asia and East Asia, and in NH winter, it is larger around Northern Australia, South Africa and South America.

4.2 Simulated MIDV: model evaluation

4.2.1 General features of simulated MIDV

A comparison of MIDV for near surface maximum temperature between the NCEP-R2 and CMIP5 model revealed that most models simulate a similar magnitude and pattern as the observed (Fig. 3), only a few models exhibit a similar pattern, but with weaker or stronger magnitude. To be more specific, the models showing a similar magnitude include ACCESS1-0, GFDL-ESM2G, HadGEM2-CC, HadGEM2-ES, and MIROC5. However, the mean of all 15 multi-model (hereinafter "MMM15") MIDV shows a similar magnitude and pattern of MIDV compared to that of the observed MIDV, regardless of the month. Kitoh and Mukano (2009) found that the CMIP3 global model ensemble underestimated mean daily temperature variability realized in the reanalysis datasets (including ERA-40, JRA-25 and NCEP–NCAR). They also stated that this was probably related to the less developed synoptic disturbances within the models than in the reanalysis datasets.

From an annual cycle of land-only areal weighted averaging of MIDV for all variables (Fig. 4), we found that models' performance in representing observed MIDV over land is consistent across all months, but the performance varies depending on the variables considered. In addition, the multi-model mean MIDV for surface maximum and minimum temperature consistently shows lower amplitude than the observed (Fig. 4a, b). The multi-model mean MIDV for surface wind speed is in good agreement with the observed MIDV (Fig. 4c). That is, the multi-model mean for MIDV for surface maximum and minimum temperature, and wind speed represents the observed MIDV (Fig. 4a–c). For precipitation, however, the observed MIDV exceeds the largest modeled MIDV as well as the multi-model mean for MIDV (Fig. 4d), which is related to the fact that precipitation is more directly tied with convection schemes and that convection parameterizations in models are far from perfect at present (e.g., Martin and Schumacher 2012; Tost et al. 2006). Adequate treatment of convection in the models is crucial for resolving the temporal variability and the intensity of total precipitation because the mean and variability of convection precipitation depend on key closure parameters of convection schemes (Lin et al. 2000; Scinocca and McFarlane 2004) and strong interaction between convective and large-scale precipitation (Scinocca and McFarlane 2004). Although considerable efforts have been made to improve convective parameterizations over the past decades, a variety of convection schemes are used in different models and each of them still has weakness (Tost et al. 2006). Also, that the MIDV for precipitation is so small may also be related to the well-known result that precipitation events in GCMs occur too often and the intensities are too light. This can make it difficult for climate models to resolve day-to-day variations in precipitation in space and time, which is expected as precipitation has a greater variability in space and time than the other variables, and thus climate models are less skillful at simulating precipitation (Alexander and Arblaster 2009). Nevertheless, several studies have suggested that it is still meaningful to utilize climate models when projecting the climate-change signal for precipitation in a future climate (e.g., Hagemann and Jacob 2007; Sushama et al. 2006). As a result, general

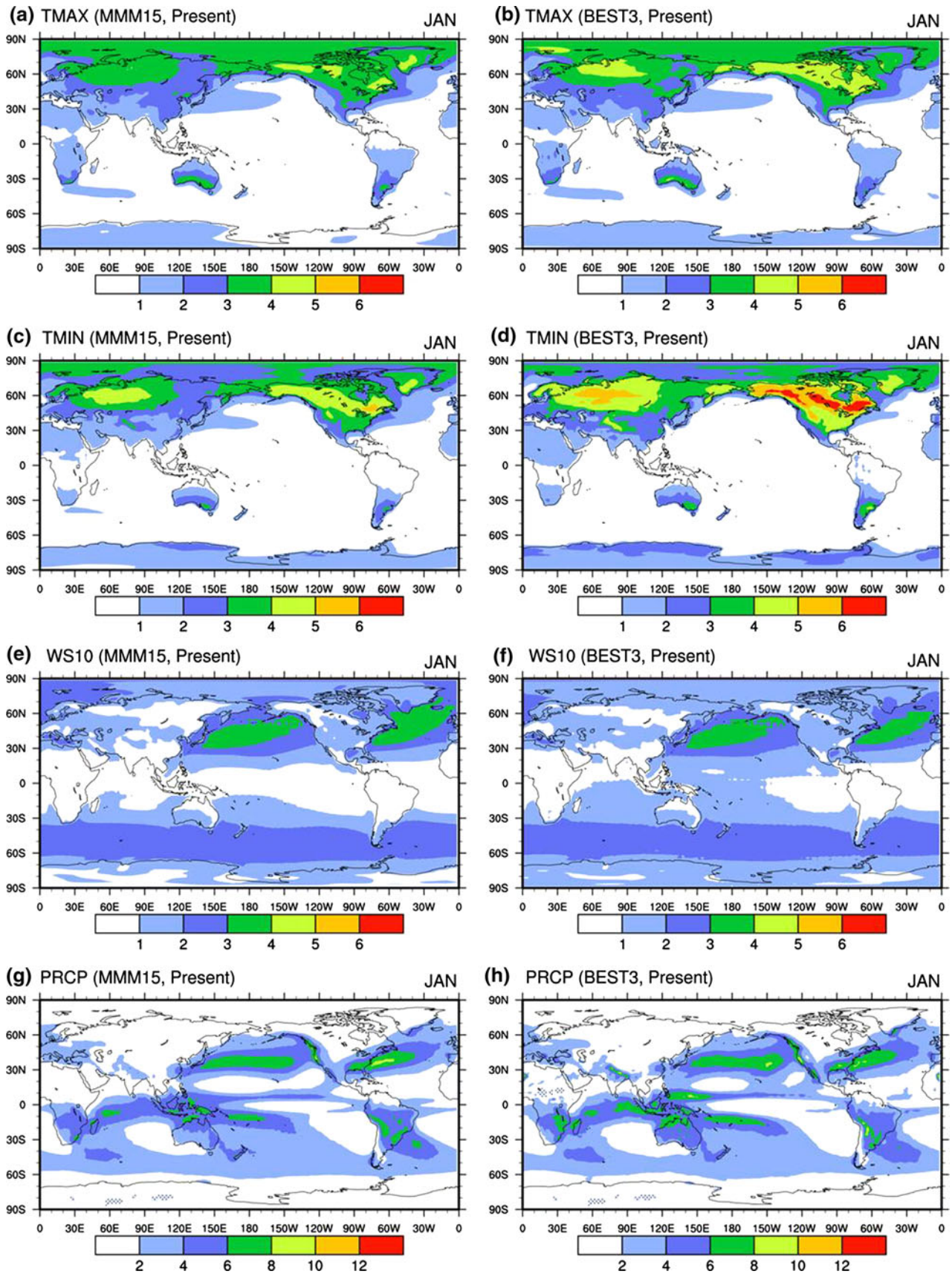

◀**Fig. 8** Simulated MIDV in **a**, **b** surface maximum temperature (K), **c**, **d** surface minimum temperature (K), **e**, **f** surface wind speed (m/s) in January for 27 years from 1979 to 2005 and **g**, **h** precipitation (mm/day) in January for 9 years from 1997 to 2005. *Left panel* is for the MIDV estimated from MMM15 and *right panel* is for MIDV from BEST3

features of the simulated MIDV (as in Fig. 3 and Fig. 4) suggest that for different variables it would be possible to select certain models which performed well in resolving observed MIDV.

4.2.2 Selection of the best models

In consideration of the observed MIDV from reanalysis and GPCP datasets as reference data, we evaluated the CMIP5 multi-models' ability to resolve the MIDV in the current climatic conditions (i.e., 1997–2005 for precipitation and 1979–2005 for other variables). In judging the models' performance based on metrics consisting of VI, PCC and RMSE, we selected the top three best models for each variable, regardless of the month.

We first examined the spatial pattern and magnitude of the variability index (VI) as one of the factors used in this study. In analyzing the spatial pattern and magnitude of the VI for maximum temperature in January we found that most models, with the exception of bcc-csm1-1 and CanESM2 exhibit a relatively small VI (Fig. 5). The bcc-csm1-1 exhibits a large VI over almost the entire ocean and CanESM2 represents a large VI mainly over the tropical ocean. We also found that within each model, the amount of VI shown depends on the variable considered.

We then assessed each factor within the metrics in order to assess the models' performance with respect to MIDV. Based on this assessment, it is expected that models showing a smaller VI, a larger PCC and a smaller RMSE would justify being labeled as performing well.

In analyzing the models' performance of the VI and PCC (Fig. 6) and VI and RMSE (Fig. 7) for MIDV, we selected the top three models which show the best ability to resolve observed MIDV for each variable. We found that for maximum temperature in January(July), MRI-CGCM3, CanESM2 and MPI-ESM-LR (MRI-CGCM3, CanESM2 and MIROC5) show a smaller VI, a larger PCC and a smaller RMSE compared to the other models, suggesting that the models demonstrate as better ability to resolve the observed MIDV (Figs. 6, 7a, b). Similarly, we also selected models showing a better ability for the other variables: CanESM2, inmcm4 and bcc-csm1-1 in January (CanESM2, HadGEM2-ES and HadGEM2-CC in July) for minimum temperature (Figs. 6, 7c, d), MIROC-ESM, bcc-csm1-1 and MPI-ESM-LR in January (HadGEM2-CC, HadGEM2-ES and MIROC-ESM-CHEM in July) for wind speed (Figs. 6, 7e–f) and MPI-ESM-LR, CSIRO-Mk3-6-0 and IPSL-CM5A-MR in January (MPI-ESM-LR, CSIRO-Mk3-6-0 and inmcm4 in July) for precipitation (Figs. 6, 7g–h), respectively.

A comparison of simulated MIDV calculated from all 15 models (MMM15) with that from top three best models (BEST3) revealed that BEST3 is in good agreement with observed MIDV (Fig. 2a) for maximum temperature in January (Fig. 8a, b). For minimum temperature, BEST3 and MMM15 show less variability in the extratropical continents of the Northern Hemisphere in January (Fig. 8c, d) compared with that of the observed variability (Fig. 2c). However, the variability of BEST3 is relatively large compared with that of MMM15 which is closer to that of the observation. In addition, MMM15 and BEST3 shows similar variability of wind speed in the North Pacific and North Atlantic Ocean in January (Fig. 8e, f) Again, the variability of BEST3 as well as MMM15 agrees fairly well with that of the observed MIDV (Fig. 2e). Unlike other variables, simulated MIDV for precipitation exhibits much less variability compared with that of observed MIDV (Fig. 2g), regardless of whether the MIDV is calculated from MMM15 or BEST3 (Fig. 8g, h). This is because of the difficulties inherent in the ability of climate models to resolve the spatio-temporal variability of precipitation (e.g., Cook and Vizy 2006; Johns et al. 2006; Lambert and Boer 2001). Nonetheless, BEST3 displayed a slightly higher variability than MMM15, especially over the central and western North Pacific Ocean, central parts of South America and some parts of Southeast Asia. To conclude, using the metrics (including VI, PCC, and RMSE), we assessed the models' performance in resolving observed MIDV for each variable. In general, the simulated MIDV calculated from the top three best models (BEST3) shows better performance compared to that of all the 15 models' means (MMM15). This indicates that (1) the metrics used in this study can be useful in assessing the models' performance; (2) based on the metrics, we can reasonably well select the best models for resolving observed MIDV; and thus (3) we can expect that the best models selected can be used to project future changes in MIDV.

4.3 Future projection

4.3.1 Near surface maximum and minimum temperature

Using the top three best models chosen for each variable, we calculated the signal-to-noise ratio of simulated MIDV in near surface maximum and minimum temperature in a future climate. It is important to consider projections for maximum and minimum temperature separately when assessing the impact of climate change, because the impact on certain societies and ecosystems will be directly related to changes in daily minimum or maximum temperature

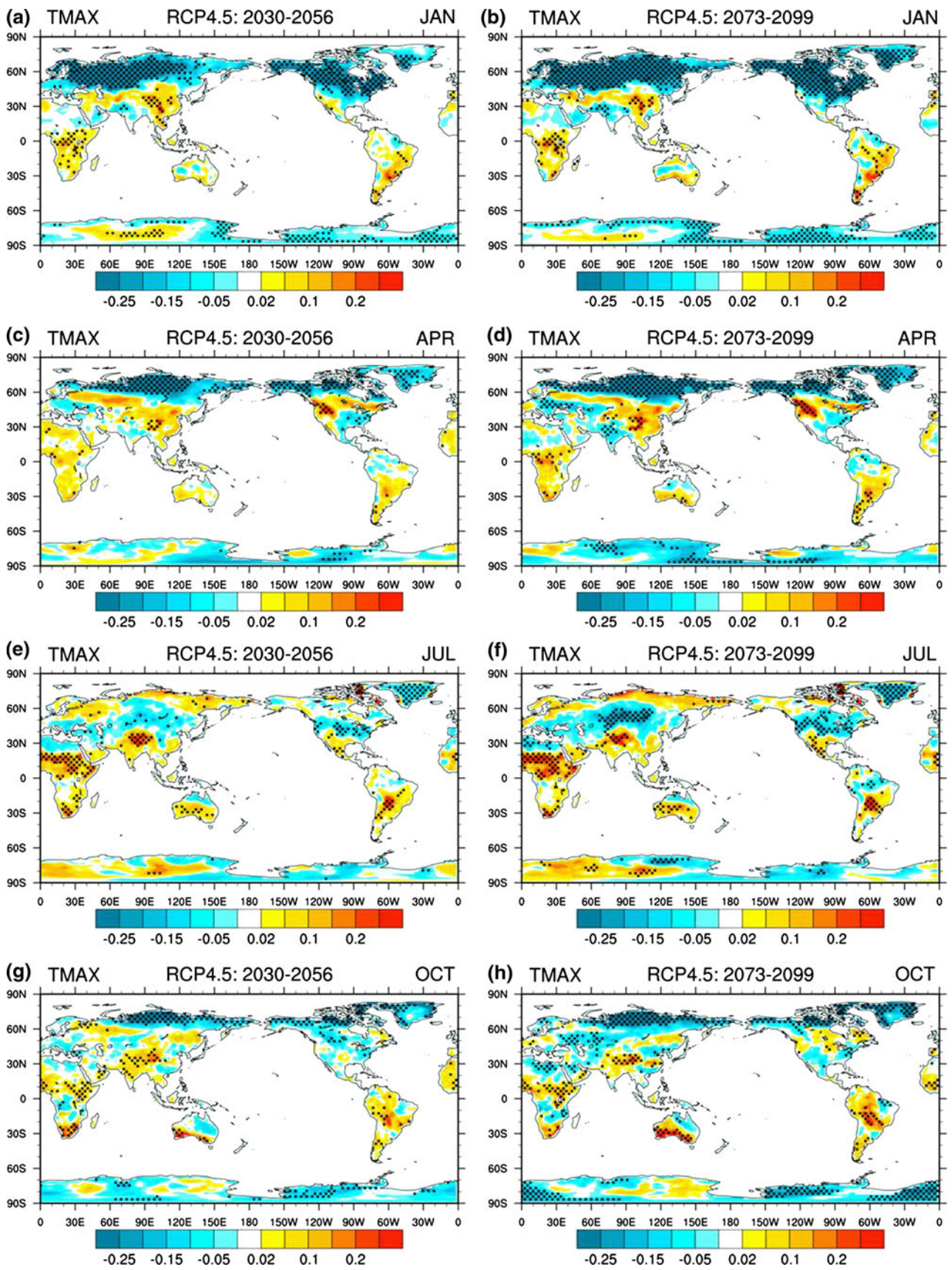

◄**Fig. 9** *Shading* indicates future projected changes in MIDV in surface maximum temperature (K) over land calculated from BEST3: **a**, **b** January, **c**, **d** April, **e**, **f** July and **g**, **h** October. The changes are given for the RCP4.5 simulation for the period 2030–2056 (mid-twenty-first century, left panel) and for the period 2073–2099 (late-twenty-first century, right panel) relative to historical simulation for the period 1979-2005. *Stippling* shows that the magnitude of BEST3 ensemble mean changes exceeds the inter-model standard deviation (i.e., the absolute value of SN ratio is greater than 1, which indicates dominance of signal over noise). Note that all ensemble members of BEST3 (see Table 1) in the RCP4.5 simulation (mid-twenty-first century and late-twenty-first century) that are consistent with those in the historical simulation are used in the calculation of the multi-model mean and inter-model standard deviation

rather than to changes in daily mean temperature (Lobell et al. 2007).

In a future climate, in the middle to high latitudes of the Northern Hemisphere in NH winter, for example over North America and the northern part of Eurasia (Figs. 9a, b, 10a, b), there is a signal of noticeable reduction in the MIDV for surface maximum and minimum temperature. The magnitude of the reduction in the MIDV for surface maximum temperature is quite similar to that of minimum temperature over these regions; indicating that the day-to-day temperature variability is projected to decrease at a similar rate during both the day and night in NH winter over those areas. Under warmer climate conditions, forced by a doubling of CO_2, the reduction of the meridional gradient of temperature in the winter high latitudes leads to a reduction in the frequency or intensity of baroclinic disturbances, and thus a reduction in the day-to-day variability of near surface temperature in the winter high latitudes where sea ice is replaced by open water (Cao et al. 1992). Unlike regions such as North America and the northern part of Eurasia, a general disparity between the surface maximum and minimum temperature uncertainty is observed in NH winter. For example, there is a generally increased signal in the MIDV for maximum temperature over the Southeast Asia and the southern part of Africa, whereas there is decreased signal in the MIDV for minimum temperature over there regions.

There is a signal of reduction of the MIDV for both maximum and minimum temperature in the high latitudes in NH spring (Figs. 9c, d, 10c, d). For maximum temperature, there is a signal of increase in the MIDV over regions such as the southern part of North America, the southern part of South America, the Southeast Asia and the southern part of Africa, whereas for minimum temperature there is decreasing change in the MIDV over those regions.

Spatial patterns of changes of the MIDV for maximum and minimum temperature in NH summer are different from those in other seasons (Figs. 9e, f, 10e, f). The models project decreasing (increasing) signal of changes in MIDV in Greenland and the southern part of North America (the northern part of India and West and East Africa. The models also show decrease in MIDV for minimum temperature over the eastern parts of Eurasia, the northern parts of Australia and the southern part of North America.

In NH autumn, there is again a signal of significant reduction in MIDV for both maximum and minimum temperature in the high latitudes, and the models project a signal of increase of the MIDV for maximum temperature over regions such as India and parts of Africa. As in other seasons, the models project large decrease in the MIDV for minimum temperature over most land parts (Figs. 9g, h, 10g, h).

In analyzing future projections of changes in simulated MIDV for both maximum and minimum surface temperature, we found that there is a signal of marked reduction in MIDV for maximum and minimum temperature over high latitudes in cold seasons. In particular, the spatial extent of reduction in MIDV covers broader areas in NH winter than in any other seasons. In addition, the models also show that there is a large increase of the MIDV for maximum temperature in many areas, but there is a larger decrease in the MIDV for minimum temperature in broad areas. Changes in advection, having a substantial influence on day-to-day temperature variability, could be one of the possible reasons for the differences in changes in the MIDV among regions (Cao et al. 1992). We also found that changes in MIDV for maximum temperature are noisy in more regions than do those for minimum temperature; suggesting the models' higher uncertainty in the MIDV projection for maximum temperature than for minimum temperature.

4.3.2 Near surface wind speed

The MIDV for surface wind speed exhibits a large uncertainty (noisy) over many areas (Fig. 11) and there is signal of future weakening throughout most of the year with the exception of NH winter. In NH winter, there is a large increase in the MIDV over the Southeast and East Asia and the northern part of India, but a reduction over Greenland and the southern part of South America (Fig. 11a, b). In NH spring, there is a significant reduction in the MIDV over broader parts of the Eurasian continent and over North America (Fig. 11c, d). Changes in MIDV for surface wind speed show more regional or local differences compared to those in surface maximum and minimum temperature. Spatial variations in changes in MIDV reflect differences in the frequency and intensity of periodic surface wind changes at the various locations.

4.3.3 Precipitation

In a future climate, there is a signal of increase in the MIDV for precipitation in the middle to high latitudes in

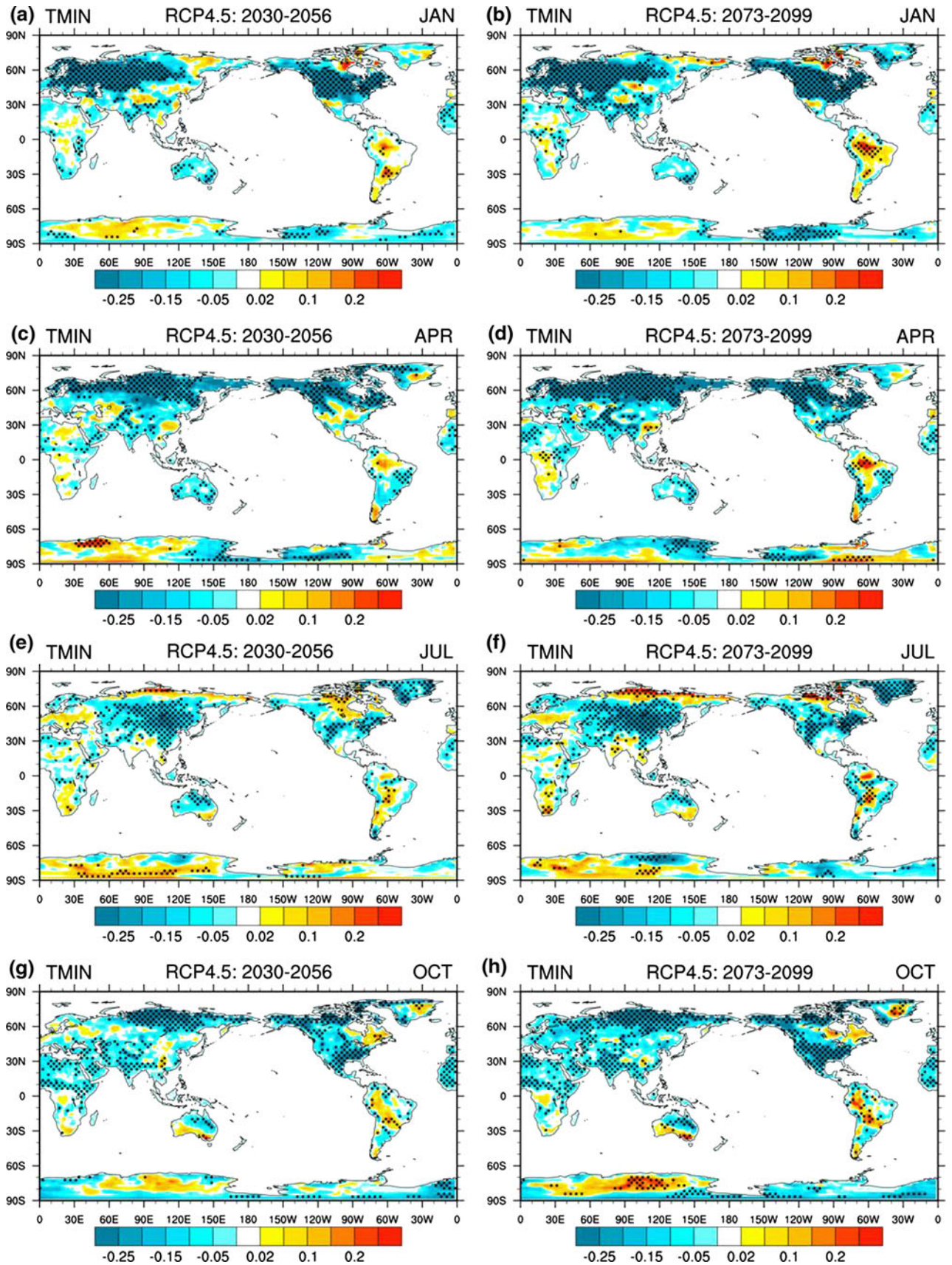

Fig. 10 Same as Fig. 9 except for surface minimum temperature (K)

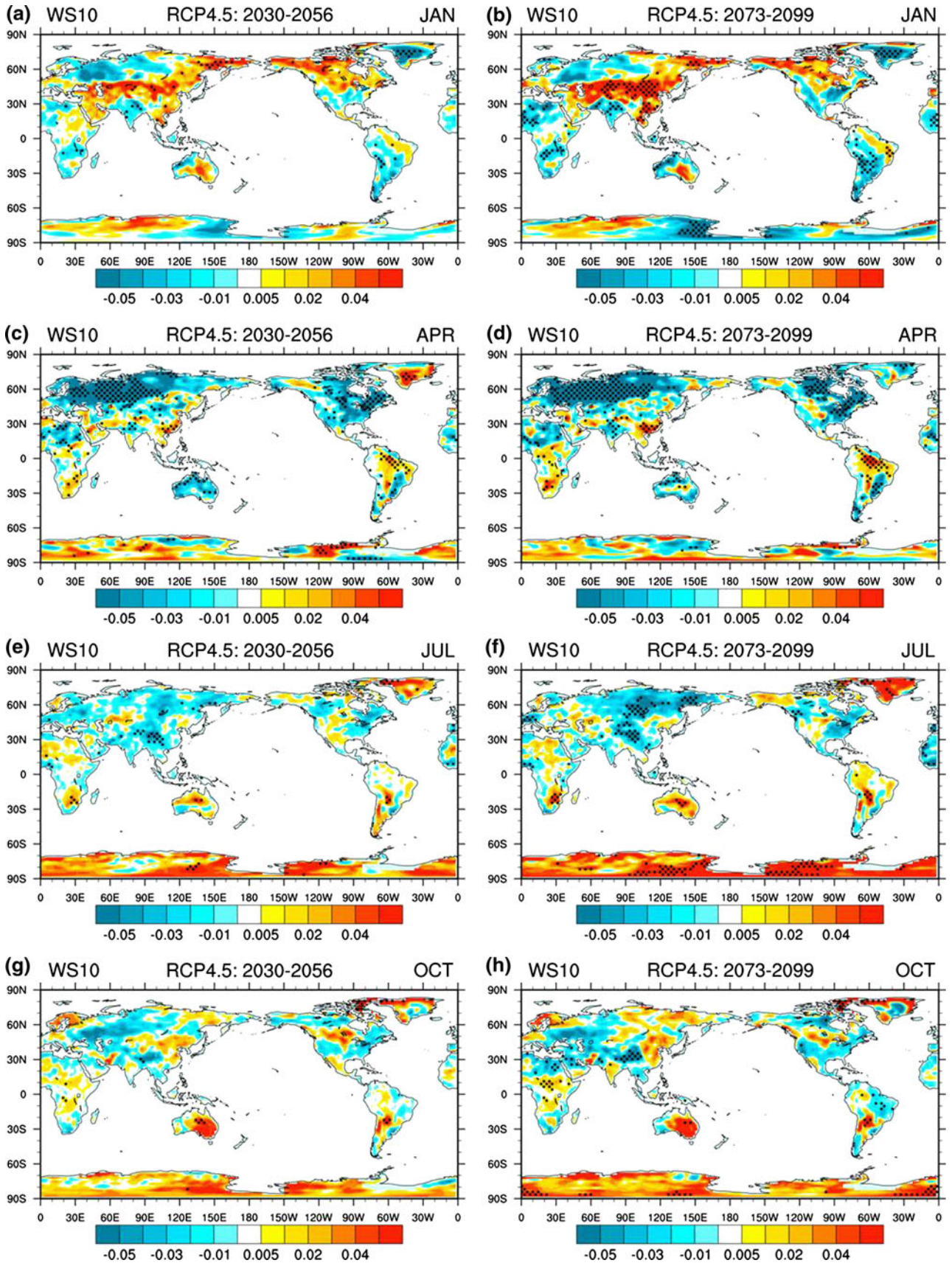

Fig. 11 Same as Fig. 9 except for surface wind speed (m/s)

the Northern Hemisphere in NH winter. This means that the models show a similar tendency (less uncertainty) of increase in the MIDV for precipitation (Fig. 12a, b) over those regions. In addition, the signal of increase is amplified in NH spring compared to in NH winter (Fig. 12c, d). In particular, there will be a strong increase in the MIDV for precipitation over North America and the continent of Eurasia with the exception of India. In NH summer, there is a signal of marked increase (decrease) in the MIDV for precipitation over East Asia, Southeast Asia, and West and East Africa (the southern part of North America), but the changes are insignificant over other regions due to high signal-to-noise ratio (Fig. 12e, f). In NH autumn, the spatial pattern is generally similar to that of NH spring (Fig. 12g, h). There will be an increase in the MIDV for precipitation over East Asia and the eastern parts of North America.

In analyzing future projections of changes in simulated MIDV for precipitation, we found that there is a noticeable signal of increase in the middle to high latitudes of the Northern Hemisphere in NH winter and spring. In particular, there is a signal of large increase in the MIDV for precipitation over East Asia and Southeast Asia throughout most of the year, suggesting that the models show a similar tendency (less uncertainty) of an increase in the MIDV for precipitation over the region. In addition, the signal of changes in MIDV for precipitation is more obvious over land in the Northern Hemisphere than in the Southern Hemisphere.

5 Summary and concluding remarks

Using a recently released, comprehensive global multi-model ensemble dataset formed by CMIP5 GCMs, we assessed the models' ability to represent MIDV for surface variables: surface maximum and minimum temperature and, surface wind speed and precipitation, under present climatic conditions (i.e., 1997–2005 for precipitation and 1979–2005 for other variables). We found that some models simulate a similar magnitude and pattern with the observed counterparts, and the remaining models showed a similar pattern but significantly weaker (or stronger) magnitude. This feature of simulated MIDV was shown for variables such as surface maximum and minimum temperature and surface wind speed throughout most of the year. However, the magnitude of simulated MIDV for precipitation was much weaker than that of the observed MIDV.

Using three different verification measures, including the pattern correlation coefficient (PCC), root-mean square error (RMSE) and variability index (VI), we also qualitatively evaluated the models' performance in their ability to represent the observed MIDV. The VI is a newly proposed measure that can quantitatively reveal how well a model can resolve the observed MIDV. Based on statistics from these three verification measures, we selected the top three models for each surface variable. As a result we chose different "best models" for different variables for a particular month. Using an ensemble mean of MIDV from the top three models chosen separately for each surface variable, we also examined the signal-to-noise ratio of simulated MIDV in a future climate.

In analyzing future projections for changes in simulated MIDV of surface maximum and minimum temperature, we found that the signal of a marked reduction in the MIDV is obvious over high latitudes, particularly in cold seasons. This reduction signal is much more noticeable in NH winter than in any other seasons. Also, the extent of reduction signal covers broader areas in minimum temperature than those in maximum temperature. The models also showed a slight increase in the MIDV for surface maximum temperature and a larger decrease for minimum temperature over some regions. In addition, we found that the models showed a higher uncertainty in the MIDV for the maximum temperature than for the minimum temperature. We found that there is a reduction in the MIDV for surface wind speed over large land areas in the NH spring than in any other seasons. In particular, a relatively clear signal of reduction is evident over the continent of Eurasia and the eastern parts of North America in NH spring. However, the models revealed large spatial variations of changes in MIDV for surface wind speed, compared with those for other surface variables. We also found that there is a signal of noticeable increase in the MIDV for precipitation over the Southeast and East Asia and the northern part of India in NH winter. In addition, there is a signal of large increase in the MIDV for precipitation over East Asia and Southeast Asia throughout most of the year.

This study suggests a possible change in the characteristics of weather (day-to-day) under future climate conditions. These changes in the features of future weather conditions should be considered as important as those of mean climate change, because the increasing risk of extremes is related to the variability on daily time scales as well as to mean climate change. For instance, most impacts of heat waves on societies and ecosystems act on daily and weekly time sales (e.g., Fischer and Schär 2009).

How to interpret the MIDV future changes? In most cases, the MIDV of minimum and maximum temperature and surface wind speed is determined by the vigorousness of the synoptic systems (Kitoh and Mukano 2009). A reduction of MIDV means weakening of the disturbances while an increase means strengthening of the synoptic systems. To understand these changes, one has to link the synoptic scale changes to the large scale environmental

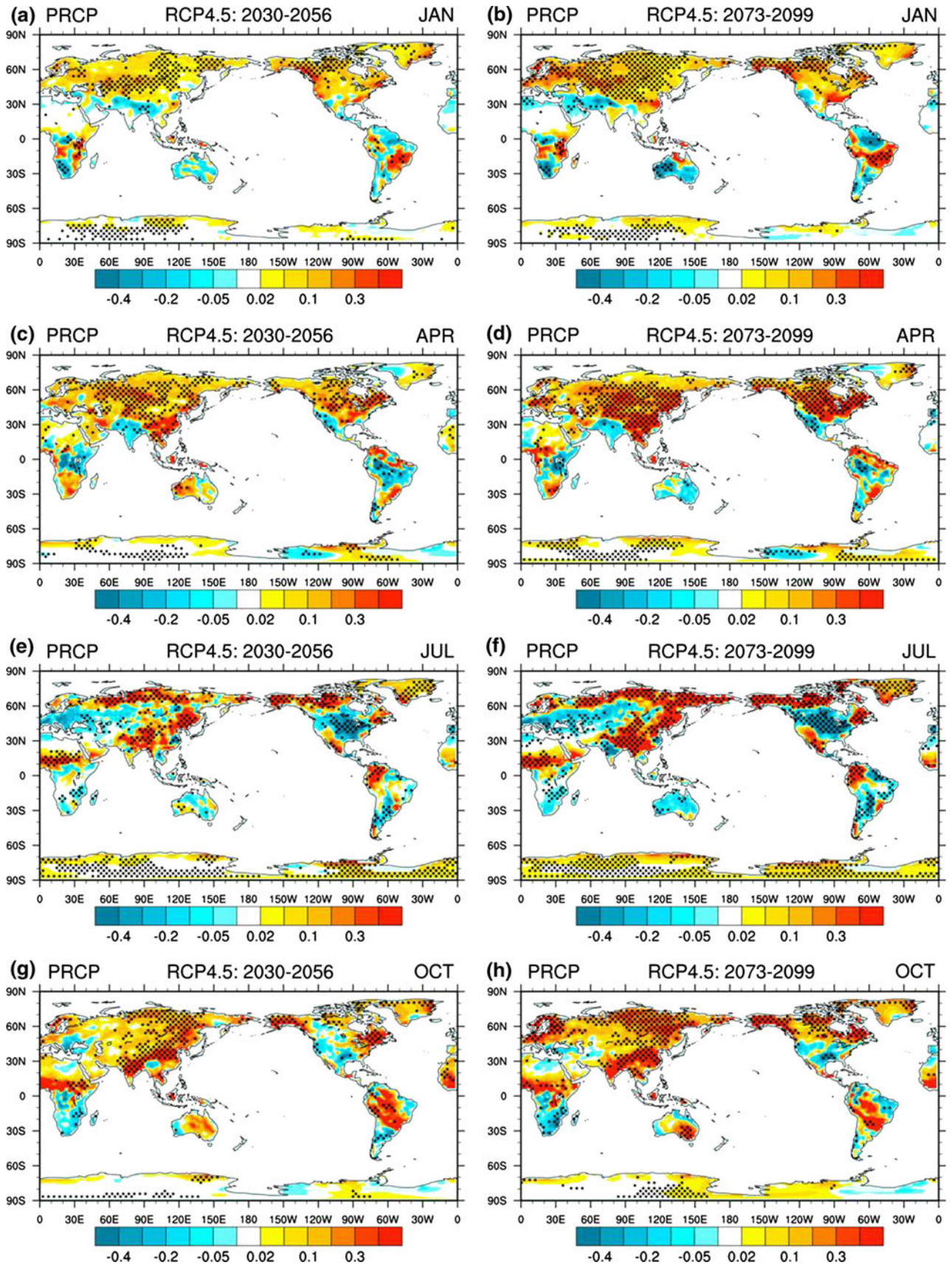

Fig. 12 Same as Fig. 9 except for precipitation (mm/day)

circulation changes (Williams and Parker 1997), such as changes in the baroclinicity in midlatitudes and the strength of the tropical convergence zones and subtropical highs as well as moisture availability in the tropics and subtropics. For precipitation, increased (reduced) MIDV is normally associated with increased (decreased) mean precipitation (Wang and Rui 1990). The mean precipitation change in future is characterized by "dry-gets-drier" and "wet-gets-wetter" (Held and Soden 2006; Neelin et al. 2006; Chou et al. 2009; Liu et al. 2013) due mainly to the increased moisture advection by mean circulation (Chou et al. 2009) and intensification of the monsoon precipitation (Wang et al. 2012; Lee and Wang 2013). "Wet-gets-wetter" implies an increase of the mean precipitation in the ITCZ and summer monsoon regions; the increased mean precipitation in turn links to increased temporal variability (MIDV) of precipitation, which is the result obtained in this study. Therefore, it is considered that future studies are needed to examine the changes in the atmospheric circulation patterns and/or synoptic disturbances associated with changes in MIDV at the surface. That is, the inclusion of phenomena that leads to large-scale atmospheric circulation or oceanic conditions could further explain the changes in day-to-day variability in a future climate. Attributing land surface processes to the MIDV on the surface would also be an important subject area for exploration in future studies.

Several other issues also remain to be solved through further in-depth studies. For example, the physical basis for the functional relationship between day-to-day variability and changes in extremes for a certain variable, are yet to be clarified. Various research has assessed the change in climate extremes (Easterling et al. 2000; Frich et al. 2002; Klein Tank and Können 2003; Alexander et al. 2006). However, few systematic and extensive studies have been conducted on the relationship between changes in extreme climatic events and day-to-day variability at the surface, even though future changes in daily variability at the surface are associated with extremes and will thus have a significant influence on our life and on several application sectors (Kitoh and Mukano 2009). Furthermore, the utilization of modeling data on a much finer spatial scale, through various dynamical and/or statistical techniques, would allow for the study of the relationship between regional or local factors and the day-to-day variability on the surface over specific areas.

Acknowledgments We acknowledge the World Climate Research Programme's Working Group on Coupled Modelling, which is responsible for CMIP, and we thank the climate modeling groups (listed in Table 1 of this paper) for producing and making available their model output. For CMIP the U.S. Department of Energy's Program for Climate Model Diagnosis and Intercomparison provides coordinating support and led development of software infrastructure in partnership with the Global Organization for Earth System Science Portals. B.W. acknowledges support provided by APEC Climate Center through Climate Prediction and its Application to Society (CliPAS) project.

References

Alexander LV, Arblaster JM (2009) Assessing trends in observed and modeled climate extremes over Australia in relation to future projections. Int J Climatol 29:417–435. doi:10.1002/joc.1730

Alexander LV, Zhang X, Peterson TC, Caesar J, Gleason B, Klein Tank AMG, Haylock M, Collins D, Trewin B, Rahimzadeh F, Tagipour A, Rupa Kumar K, Revadekar J, Griffiths G, Vincent L, Stephenson DB, Burn J, Aguilar E, Brunet M, Taylor M, New M, Zhai P, Rusticussi M, Vazquez-Aguirre JL (2006) Global observed changes in daily climate extremes of temperature and precipitation. J Geophys Res 111. doi:10.1029/2005JD006290

Bolvin DT, Adler RF, Huffman GJ, Nelkin EJ, Poutiainen JP (2009) Comparison of GPCP monthly and daily precipitation estimates with high-latitude gauge observations. J Appl Meteorol Climatol 48:1843–1857

Cao HX, Mitchell JFB, Lavery JR (1992) Simulated diurnal range and variability of surface temperature in a global climate model for present and doubled CO_2 climates. J Clim 5:920–943

Chou C, Neelin JD, Chen CA, Tu JY (2009) Evaluating the "rich-get-richer" mechanism in tropical precipitation change under global warming. J Clim 22:1982–2005

Clarke LE, Edmonds JA, Jacoby HD, Pitcher H, Reilly JM, Richels R (2007) Scenarios of greenhouse gas emissions and atmospheric concentrations. Sub-report 2.1a of Synthesis and Assessment Product 2.1. Climate Change Science Program and the Subcommittee on Global Change Research, Washington DC

Cook KH, Vizy EK (2006) Coupled model simulations of the West African monsoon system: 20th century simulations and 21st century predictions. J Clim 19:3681–3703

Dee DP, Uppala SM, Simmons AJ, Berrisford P, Poli P, Kobayashi S, Andrae U, Balmaseda MA, Balsamo G, Bauer P, Bechtold P, Beljaars ACM, van de Berg L, Bidlot J, Bormann N, Delsol C, Dragani R, Fuentes M, Geer AJ, Haimberger L, Healy SB, Hersbach H, Hólm EV, Isaksen L, Kållberg P, Köhler M, Matricardi M, McNally AP, Monge-Sanz BM, Morcrette J–J, Park BK, Peubey C, de Rosnay P, Tavolato C, Thépaut J-N, Vitart F (2011) The ERA-Interim reanalysis: configuration and performance of the data assimilation system. Q J R Meteorol Soc 137:553–597. doi:10.1002/qj.828

Deser C, Phillips A, Bourdette V, Teng H (2012) Uncertainty in climate change projections: the rule of internal variability. Clim Dyn 38:527–546. doi:10.1007/s00382-010-0977-x

Driscol DM, Rice PB, Fong JMY (1994) Spatial variation of climatic aspects of temperature: interdiurnal variability and lag. Int J Climatol 14:1001–1008. doi:10.1002/joc.3370140905

Easterling DR, Evans JL, Groisman PY, Karl TR, Kenkel KE, Ambenje P (2000) Observed variability and trends in extreme climate events: a brief review. Bull Am Meteorol Soc 81:417–425

Fischer EM, Schär C (2009) Future changes in daily summer temperature variability: driving processes and role for temperature extremes. Clim Dyn 33:917–935

Frich PL, Alexander V, Della-Marta P, Gleason B, Haylock M, Klein Tank AMG, Peterson T (2002) Observed coherent changes in climate extremes during the second half of the twentieth century. Clim Res 19:193–212

Gebremichael M, Krajewski WF, Morrissey ML, Huffman GJ, Adler RF (2005) A detailed evaluation of GPCP 1° daily rainfall

estimates over the Mississippi River Basin. J Appl Meteorol 44:665–681
Gleckler PJ, Taylor KE, Doutriaux C (2008) Performance metrics for climate models. J Geophys Res 113:D06104. doi:10.1029/2007JD008972
Hagemann S, Jacob C (2007) Gradient in the climate change signal of European discharge predicted by a multi-model ensemble. Clim Change 81:309–327
Held IM, Soden BJ (2006) Robust responses of the hydrological cycle to global warming. J Clim 19:5686–5699
Hibbard KA, Meehl GA, Cox P, Friedlingstein P (2007) A strategy for climate change stabilization experiments. EOS 88:217, 219, 221
Huffman GJ, Adler RF, Morrissey MM, Curtis S, Joyce R, McGavock B, Susskind J (2001) Global precipitation at one-degree daily resolution from multi-satellite observations. J. Hydrometeorol 2:36–50
IPCC (2007) Climate change 2007: the physical science basis. In: Solomon S, Qin D, Manning M, Chen Z, Marquis M, Averyt KB, Tignor M, Miller HL (eds) Contribution of working group I to the fourth assessment report of the IPCC. Cambridge University Press, Cambridge, United Kingdom and New York, NY, USA
Johns TC, Durman CF, Banks HT, Robert MJ, McLaren AJ, Ridley JK, Senior CA, Williams KD, Jons A, Richard GJ, Cusack S, Ingram WJ, Crucifix M, Sexton DMH, Joshi MM, Dong BW, Spencer H, Hill RSR, Gregory JM, Keen AB, Pardaens AK, Lowe JA, Bodas-Salcedo A, Stark S, Searl Y (2006) The new Hadley center climate model (HadGEM1): evaluation of coupled simulations. J Clim 19:1327–1353
Kanamitsu M, Ebisuzaki W, Woolen J, Yang SK, Hnilo JJ, Fiorino M, Potter GL (2002) NCEP–DOE AMIP-II reanalysis (R-2). Bull Am Meteorol Soc 83:1631–1643
Kitoh A, Mukano T (2009) Changes in daily and monthly surface air temperature variability by multi-model global warming experiments. J Meteorol Soc Jpn 87:513–524
Klein Tank AMG, Können GP (2003) Trends in indices of daily temperature and precipitation extremes in Europe, 1946–99. J Clim 16:3665–3680
Lambert SJ, Boer GJ (2001) CMIP1 evaluation and intercomparison of coupled climate models. Clim Dyn 17:83–106
Lee JY, Wang B (2013) Future change of global monsoon in the CMIP5. Clim Dyn 39:1123–1135. doi:10.1007/s00382-012-1564-0
Lin X, Randall DA, Fowler LD (2000) Diurnal variability of the hydrologic cycle and radiative fluxes: comparisons between observations and a GCM. J Clim 13:4159–4179
Liu J, Wang B, Cane MA, Yim SY, Lee JY (2013) Divergent global precipitation changes induced by natural and anthropogenic forcing. Nature 493:656–659
Lobell DB, Bonfils C, Duffy PB (2007) Climate change uncertainty for daily minimum and maximum temperatures: a model intercomparison. Geophys Res Lett 34:L05715. doi:10.1029/2006GL028726
Martin ER, Schumacher C (2012) The relationship between tropical warm pool precipitation, sea surface temperature, and large-scale vertical motion in IPCC AR4 models. J Atmos Sci 69:185–194
Meehl GA, Hibbard KA (2007) A strategy for climate change stabilization experiments with AOGCMs and ESMs. WCRP Informal Report No. 3/2007, ICPO Publication No. 112, IGBP Report No. 57. World Climate Research Programme, Geneva, p 35
Neelin JD, Munnich M, Su H, Meyerson JE, Holloway CE (2006) Tropical drying trends in global warming models and observations. Proc Natl Acad Sci USA 103:6110–6115
Pincus R, Batstone CP, Hofmann JP, Taylor KE, Glecker PJ (2008) Evaluating the present-day simulation of clouds, precipitation, and radiation in climate models. J Geophys Res 113:D14209. doi:10.1029/2007JD009334
Prudhomme C, Reynard N, Crooks S (2002) Downscaling of global climate models for flood frequency analysis: where are we now? Hydrol Process 16:1137–1150
Rosenthal SL (1960) The interdiurnal variability of surface-air temperature over the north Atlantic ocean. J Meteorol 17:1–7
Santer BD, Mears C, Doutriaux C, Caldwell P, Gleckler PJ, Wigley TML, Solomon S, Gillett NP, Ivanova D, Karl TR, Lanzante JR, Meehl GA, Stott PA, Taylor KE, Thorne PW, Wehner MF, Wentz FJ (2011) Separating signal and noise in atmospheric temperature changes: the importance of timescale. J Geophys Res 116:D22105. doi:10.1029/2011JD016263
Scherrer SC (2011) Present-day interannual variability of surface climate in CMIP3 models and its relation to future warming. Int J Climatol 31:1518–1529. doi:10.1002/joc.2170
Scinocca J, McFarlane NA (2004) Variability of modelled tropical precipitation. J Atmos Sci 61(16):1993–2015
Smith SJ, Wigley TML (2006) MultiGas forcing stabilization with minicam. Energy J Special issue 3#:373–392
Sushama L, Laprise R, Caya D, Frigon A, Slivitzky M (2006) Canadian RCM projected climate-change signal and its sensitivity to model errors. Int J Climatol 26:2141–2159
Szczypta C, Calvet J-C, Albergel C, Balsamo G, Boussetta S, Carrer D, Lafont S, Meurey C (2011) Verification of the new ECMWF ERA-Interim reanalysis over France. Hydrol Earth Syst Sci 15:647–666. doi:10.5194/hess-15-647-2011
Taylor KE (2001) Summarizing multiple aspects of model performance in a single diagram. J Geophys Res 106:7183–7192
Taylor KE, Stouffer RJ, Meehl GA (2012) An overview of CMIP5 and the experiment design. Bull Am Meteorol Soc 93:485–498. doi:10.1175/BAMS-D-11-00094.1
Tost H, Jöckel P, Lelieveld J (2006) Influence of different convection parameterizations in a GCM. Atmos Chem Phys 6:5475–5493
Wang B, Rui H (1990) Synoptic climatology of transient tropical intraseasonal convection anomalies. Meteorol Atmos Phys 44(1–4):43–61
Wang B, Liu J, Kim HJ, Webster PJ, Yim SY (2012) Recent change of the global monsoon precipitation (1979–2008). Clim Dyn 39:1123–1135. doi:10.1007/s00382-011-1266-z
Williams KRS, Parker KC (1997) Trends in interdiurnal temperature variation for the central United States, 1945–1985. Prof Geogr 49:342–355. doi:10.1111/0033-0124.00082
Wise M, Calvin K, Thomson A, Clarke L, Bond-Lamberty B, Sands R, Smith SJ, Janetos A, Edmonds J (2009) Implications of limiting CO2 concentrations for land use and energy. Science 324:1183–1186
Yin X, Gruber A, Arkinc P (2004) Comparison of the GPCP and CMAP merged gauge-satellite monthly precipitation products for the period 1979–2001. J Hydrometeorol 5:1207–1222